

Off-axis stability of intense continuous relativistic beams

Luciano C. Martins, Felipe B. Rizzato, and Renato Pakter

Citation: *Journal of Applied Physics* **106**, 043305 (2009); doi: 10.1063/1.3204972

View online: <http://dx.doi.org/10.1063/1.3204972>

View Table of Contents: <http://scitation.aip.org/content/aip/journal/jap/106/4?ver=pdfcov>

Published by the [AIP Publishing](#)



Re-register for Table of Content Alerts

Create a profile.



Sign up today!



Off-axis stability of intense continuous relativistic beams

Luciano C. Martins,^{1,2} Felipe B. Rizzato,¹ and Renato Pakter^{1,a)}

¹*Instituto de Física, Universidade Federal do Rio Grande do Sul, Caixa Postal 15051, 91501-970 Porto Alegre, Rio Grande do Sul, Brazil*

²*Departamento de Física, Universidade do Estado de Santa Catarina, 89223-100 Joinville, Santa Catarina, Brazil*

(Received 30 March 2009; accepted 22 July 2009; published online 24 August 2009)

This paper investigates the stability of off-axis continuous intense relativistic beams propagating inside a circular conducting pipe. The equations of motion for the centroid and the envelope of slightly off-axis beams are derived and used to determine equilibrium and stability conditions for the beam transport. It is shown that depending on the parameters of the system, beams propagating along the pipe axis may become unstable due to the presence of the wall, imposing a fundamental limitation in the effective area that an equilibrium beam can occupy inside the conductor. © 2009 American Institute of Physics. [DOI: 10.1063/1.3204972]

I. INTRODUCTION

A better understanding of the equilibrium and stability properties in the transport of magnetically focused high-current beams is fundamental to the development of high-intensity accelerators and vacuum electronic devices. These devices are necessary to meet the needs in areas such as communication, heavy-ion fusion, and basic science research.^{1,2} In that regard, a matter of recent interest is to investigate the physics of beams displaying some misalignment with respect to the symmetry axis of the focusing field.^{3–6} Small deviations between the beam injection direction and the focusing field axis may drive off-axis beam dynamics that are potentially hazardous to the transport. Off-axis dynamics can ultimately lead to collision between the charges and the conducting walls surrounding the system, causing particle beam losses, activation of the walls,⁷ and pulse shortening in high-power microwave sources.⁸

For the particular case of intense, continuous, and round beams propagating with nonrelativistic velocities throughout a conducting cylindrical pipe, it has been shown that despite the occurrence of an unstable orbit in the centroid dynamics of off-axis beams,³ this orbit alone cannot be responsible for pushing rms matched beams toward the wall.⁶ It was also found that there is virtually no coupling between the centroid oscillation and the beam particles dynamics, which prevents conversion of the centroid motion energy into beam particles thermalization and the overall degradation of the beam quality.⁶ These results indicate that off-axis dynamics do not impose severe limitations in the transport of such beams.

If we now consider beams propagating with relativistic velocities, the scenario may change significantly. For relativistic beams, the electrostatic repulsive force between particles of the beam is partially screened by the attractive magnetic force imposed by the beam currents. However this screening does not occur for the interaction with the image charges *produced* by the presence of the conductor because the conductor is completely *permeable* to the magnetic field

generated by the beam current. As a consequence, the net effect of the conductor is enhanced for relativistic beams. This is true not only for *ideal* continuous beams but, more generally, whenever the pulse duration of the beam is long compared to the magnetic diffusion time $\tau_m \sim \mu\sigma d^2/c^2$ (in Gaussian units), where μ , σ , and d are, respectively, the magnetic permeability, the conductivity, and the thickness of the conductor wall, and c is the speed of light in vacuum.⁹

In this paper we investigate off-axis dynamics for such relativistic beams. The equations of motion for the centroid and the envelope of slightly off-axis beams are derived and used to determine equilibrium and stability conditions for beam transport. In particular, it is shown that depending on beam and focusing channel parameters, the system symmetry axis may become unstable due to the presence of the wall. In this case, any misalignment in the injection would lead to beam loss. It is shown that this instability imposes a fundamental limitation in the effective area that an equilibrium beam can occupy inside the conductor.

The paper is organized as follows. In Sec. II we introduce the model and the corresponding equations of motion for the beam particles. In Sec. III, we derive the dynamical equations for the centroid and envelope of the beam; a stability condition for off-axis beams is obtained. In Sec. IV, we obtain the critical value of the envelope of the beam, above which we cannot find stable beam propagation anymore and test it against results from self-consistent N -particle simulations. Finally, in Sec. V, we conclude the paper.

II. MODEL

We consider an unbunched beam propagating with a constant axial velocity $\beta_b c$ along the inner channel of a circular grounded conducting pipe of radius r_w ; the beam is focused by a uniform solenoidal magnetic field of magnitude B_z . Both pipe and focusing field are aligned with the z axis. Given the uniform motion along z , we define a longitudinal coordinate $s = \beta_b c t$ that plays the role of time in the system and investigate the transverse beam evolution as a function of s . The transverse beam density profile $n_b(\mathbf{r}, s)$ is assumed

^{a)}Electronic mail: pakter@if.ufrgs.br.

to be axisymmetric with respect to its centroid located at $\mathbf{r}_0(s) = \langle \mathbf{r} \rangle$, where \mathbf{r} is the transverse position vector measured from the center of the conducting pipe and $\langle \rangle$ means average over beam distribution. Since we are interested in the stability of the centroid motion, the beam is allowed to be slightly off-axis.

In the Larmor frame of reference,¹⁰ the dynamical equation that dictates the evolution of a beam particle can be written as

$$\mathbf{r}'' = -\sigma_0^2 \mathbf{r} - \nabla \psi_d - \nabla \psi_i, \quad (1)$$

where the prime denotes derivative with respect to s and ∇ operates on the transverse coordinates only. The first term in the right-hand side of Eq. (1) is the focusing force, with $\sigma_0 = qB_z/2\gamma_b\beta_b mc^2$ being the vacuum phase advance per unit axial length, which measures the focusing field strength, and q , m , and $\gamma_b = (1 - \beta_b^2)^{-1/2}$ are, respectively, the charge, mass, and relativistic factor of the beam particles. The second term corresponds to the direct interaction with the other beam particles, disregarding wall effects. It takes into account both self-electric and self-magnetic interactions. The self-potential ψ_d is determined by the Poisson equation

$$\nabla^2 \psi_d = -\frac{2\pi K}{N_b} n_b(\mathbf{r}, s) \quad (2)$$

in the absence of boundaries, where $K = 2q^2 N_b / \gamma_b^3 \beta_b^2 mc^2$ is the beam perveance that measures the space-charge interaction and $N_b = \int n_b d\mathbf{r} = \text{const.}$ is the number of particles per unit axial length. Finally, the third term is due to the image charges generated by the presence of the conductor walls. Once Eq. (2) has been solved for ψ_d , the potential ψ_i can in general be determined using an inversion technique.¹¹ Nevertheless, in the beam configuration analyzed here, one can readily compute ψ_i by noting that outside of an axially symmetric charge distributions, its equipotentials are identical to the equipotentials of a beam with vanishing transverse dimensions—a line of charge. Therefore, from the point of view of the pipe, the beam behaves like a line of charge located at \mathbf{r}_0 , whose image is located outside the pipe at $\mathbf{r}_i = (r_w/r_0)^2 \mathbf{r}_0$. The image potential is then given by

$$\psi_i(\mathbf{r}, s) = \gamma_b^2 K \log \left| \mathbf{r} - \frac{r_w^2}{r_0^2} \mathbf{r}_0(s) \right|. \quad (3)$$

Note that Eq. (3) is independent of the specific form of n_b and is valid for any \mathbf{r}_0 as long as the beam density profile is axisymmetric with respect to its centroid. The γ_b^2 factor appears in Eq. (3) precisely because the conductor is a boundary for the self-electric field but is not for self-magnetic field.

III. CENTROID AND ENVELOPE DYNAMICS

By taking the average of Eq. (1) over the beam distribution, we obtain an equation for the evolution of the centroid. The equation reads

$$\mathbf{r}_0'' = -\sigma_0^2 \mathbf{r}_0 - \langle \nabla \psi_d \rangle - \langle \nabla \psi_i \rangle. \quad (4)$$

As shown in Ref. 4, because of momentum conservation the average self-field interaction $\langle \nabla \psi_d \rangle$ exactly vanishes. As for the contribution from the induced charge at the conductor,

we can explicitly calculate $\langle \nabla \psi_i \rangle$ to find that as long as n_b is axisymmetric with respect to \mathbf{r}_0 , centroid and image-charge interact like attracting lines of charge located at \mathbf{r}_0 and \mathbf{r}_i , respectively. Details of the calculations are presented in the Appendix. Since we are interested in the stability at the focusing channel symmetry axis $r=0$, we retain only linear terms in \mathbf{r}_0 to find

$$\mathbf{r}_0'' = \left(-\sigma_0^2 + \frac{\gamma_b^2 K}{r_w^2} \right) \mathbf{r}_0. \quad (5)$$

From Eq. (5) it is clear that whenever the beam perveance exceeds a critical value,

$$K > \frac{\sigma_0^2 r_w^2}{\gamma_b^2}, \quad (6)$$

the beam will become unstable, with its centroid continuously moving away from the focusing field symmetry axis. A more detailed analysis of the centroid nonlinear dynamics reveals that the onset of the instability is due to a bifurcation of the equilibrium solution $\mathbf{r}_0=0$ caused by a collision with an unstable fixed point already present in the nonrelativistic case.^{3,6,12} In Ref. 9 an analogous stability condition was derived for the trajectory of a single particle located at the centroid position. In that regard, Eq. (5) is more stringent because it shows that the beam as a whole will depart from the conducting pipe center when the instability condition is met. In any case, as will be shown, depending on the beam parameters this condition may not be achieved; one still needs to investigate the beam transverse size as well in order to determine the relevance of the instability.

The effective transverse size can be measured by the beam envelope defined as $r_b = [2\langle r^2 \rangle]^{1/2}$. Taking the second derivative of r_b with respect to s and using Eq. (1), one can readily obtain an equation for the envelope evolution as

$$r_b'' = -\sigma_0^2 r_b + \frac{\epsilon^2}{r_b^3} - \frac{2}{r_b} \langle \mathbf{r} \cdot \nabla \psi \rangle, \quad (7)$$

where $\epsilon \equiv 2[\langle r^2 \rangle \langle r'^2 \rangle - \langle r r' \rangle^2]^{1/2}$ is the beam emittance and $\psi \equiv \psi_d + \psi_i$. In principle one needs to specify the transverse beam density profile in order to compute the space-charge contribution $\langle \mathbf{r} \cdot \nabla \psi \rangle$ in Eq. (7). Nevertheless, using Poisson equation (2) it is possible to eliminate the explicit dependence on $n_b(\mathbf{r}, s)$ and write¹⁰

$$\langle \mathbf{r} \cdot \nabla \psi \rangle = -\frac{1}{4\pi K} \int_0^{2\pi} \left[\left(r \frac{\partial \psi}{\partial r} \right)^2 - \left(\frac{\partial \psi}{\partial \theta} \right)^2 \right]_{r=r_w} d\theta, \quad (8)$$

where θ is the angular variable in polar coordinates. Equation (8) shows that in order to determine $\langle \mathbf{r} \cdot \nabla \psi \rangle$, we only need to specify the potential ψ along the conductor boundary. Taking advantage again of the fact that outside of the beam it behaves just like a line of charge, we can simply substitute in Eq. (8) the potential generated by two lines of charge, one corresponding to the beam located at \mathbf{r}_0 and the other to its image located at \mathbf{r}_i . With that, we can readily evaluate the integral to find

$$\langle \mathbf{r} \cdot \nabla \psi \rangle = -\frac{K}{2} \left(1 + \frac{2\gamma_b^2 r_0^2}{r_w^2 - r_0^2} \right). \quad (9)$$

Hence, the overall effect of the pipe on beams that are displaced from the center is to enhance the effective space-charge force on r_b . However, Eq. (9) shows that the dependence of $\langle \mathbf{r} \cdot \nabla \psi \rangle$ on the centroid is, to leading order, proportional to $(r_0/r_w)^2$. Because we are interested in the stability of slightly off-axis beams, this dependence can be safely disregarded, and Eq. (7) turns into

$$r_b'' = -\sigma_0^2 r_b + \frac{\epsilon^2}{r_b^3} + \frac{K}{r_b}, \quad (10)$$

whose form is identical to that of round beams. This shows that the initial assumption on the axial symmetry of $n_b(\mathbf{r}, s)$ is accurate. Actually, this detachment between envelope and centroid dynamics is corroborated by self-consistent numerical simulations that show that even in the case of beams presenting *large* amplitude centroid motion, the envelope is mostly insensitive to it.⁶

IV. CRITICAL ENVELOPE

From Eq. (10) we can determine an equilibrium state for which the beam envelope remains constant as the beam propagates: the so-called matched beam condition. This state is most desirable in practical beam transport devices because it prevents emittance growth, halo formation, and, ultimately, beam losses.^{6,10,13-17} Setting $r_b''=0$ in Eq. (10) and solving for the perveance, we obtain

$$K = \frac{\sigma_0^2 r_b^4 - \epsilon^2}{r_b^2}. \quad (11)$$

Substituting Eq. (11) in the instability condition for the centroid motion, Eq. (6), we can define a critical envelope radius

$$r_b^* = \frac{r_w}{2^{1/2}} \left[\frac{1}{\gamma_b^2} + \left(\frac{1}{\gamma_b^4} + \frac{4\epsilon^2}{\sigma_0^2 r_w^4} \right)^{1/2} \right]^{1/2}, \quad (12)$$

above which an equilibrium beam loses its stability, departing from the pipe center axis. It is worth noting that since the image effects given by ψ_i in Eq. (3) are independent of the specific form of n_b and consequently of the beam transverse size, it may sound contradictory that the presence of the conducting wall introduces a critical envelope radius in the beam transport. However, the matched condition expressed in Eq. (11) imposes a certain relation among the parameters of the system, which can be readily used to translate the critical perveance of Eq. (6) into the above stability criterion on the beam envelope. In Fig. 1, it is shown r_b^* as a function of β_b for two distinct values of the emittance: a fully space-charge dominated beam with $\epsilon=0$ (solid curve) and a finite emittance beam with $\epsilon=0.3\sigma_0 r_w^2$ (dashed curve). The region below each curve corresponds to stable beam propagation for the given emittance, whereas envelope values above the curve mean that off-axis motion is unstable. It is clear in Fig. 1 that operating with beams of higher emittance tends to raise the r_b^* curve, decreasing the instability region in the parameter space. In fact, an inspection of Eq. (12) reveals that relatively tenuous beams with $\epsilon > \sigma_0 r_w^2$ are not subjected

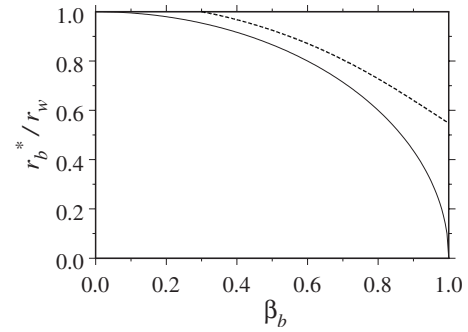


FIG. 1. Normalized critical envelope radius above which beam transport becomes unstable as function of β_b for $\epsilon=0.0$ (solid) and $\epsilon=0.3\sigma_0 r_w^2$ (dashed).

to the off-axis instability, irrespective of the value of β_b . The figure also shows that for nonrelativistic beams with $\beta_b \rightarrow 0$, the transport is always stable, in agreement with previous analysis that showed that off-axis instability is not relevant for such beams.⁶ However, as β_b is increased the instability may set in for certain values of r_b and pose severe limitations on the maximum area that the beam can occupy inside the pipe. In particular, as we move toward more intense and relativistic beams with $\epsilon \rightarrow 0$ and $\beta_b \rightarrow 1$, the instability is virtually always present, irrespective to the beam transverse size.

In order to verify the occurrence of the instability and the limitation it imposes on the beam transport, we perform self-consistent particle simulations. In the simulations, $N=5000$ macroparticles are launched according to a waterbag distribution¹⁰ with the prescribed envelope and emittance and evolve according to the force Eq. (1). The self-fields are calculated using a Green-function method.⁶ The centroid of the particle distribution is set to be at the pipe center, but due to the finite number of particles, a small r_0 arises; this serves as the seed for any instability to occur. Results showing the evolution of the centroid in the simulations are shown in Fig. 2 for $\epsilon=0$ (panel a) and $\epsilon=0.3\sigma_0 r_w^2$ (panel b). The solid (dashed) curves correspond to beams with envelopes slightly below (above) the critical envelope, namely, $r_b=0.98r_b^*$ ($r_b=1.02r_b^*$). It is clear that for the beams with $r_b < r_b^*$, the centroid motion is stable with no growth in its amplitude. These simulations were run up to large axial distances $s=1000.0$, the stability was found to be preserved, and no particle loss was detected. On the other hand, in agreement with the theory, for beams with envelopes above the critical value, r_0 grows and the beam eventually hits the wall. This leads to a complete beam loss, confirming the fundamental limitations on the transverse beam sizes imposed by the instability.

V. CONCLUSION

We have investigated the off-axis stability of intense relativistic beams propagating inside a circular conducting pipe. The equations of motion for the centroid and the envelope of slightly off-axis beams were derived and used to determine equilibrium and stability conditions for the beam transport. It was shown that there exists a critical transverse effective size of the beam, above which the centroid dynamics becomes unstable. In this case, beams that are injected

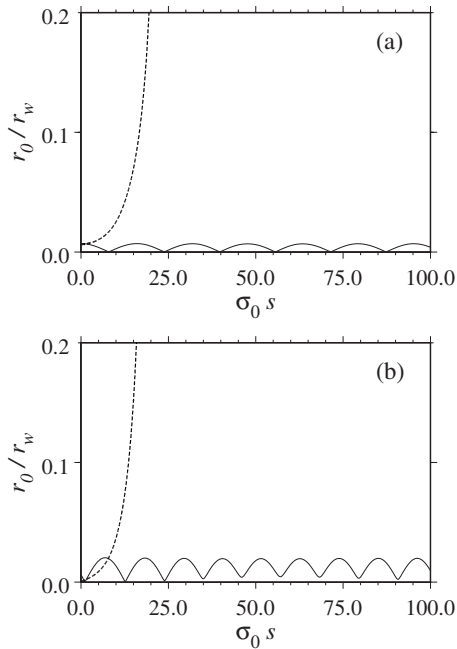


FIG. 2. Evolution of the centroid in self-consistent simulations for beams with initial envelopes slightly below $r_b=0.98r_b^*$ (solid) and above $r_b=1.02r_b^*$ (dashed) the critical envelope in Eq. (12). In (a), $\epsilon=0.0$ and $\beta_b=0.7$, and in (b), $\epsilon=0.3\sigma_0 r_w^2$ and $\beta_b=0.8$.

with any small misalignment are driven toward the wall, leading to beam loss. This imposes a fundamental limitation in the effective area that an equilibrium beam can occupy inside the conductor. Self-consistent simulations confirm the results from the theory.

ACKNOWLEDGMENTS

The authors thank Pedro Tavares for interesting discussions on relativistic aspects of beam propagation. This work was supported by CNPq, Brazil, and by the U.S.-AFOSR under Grant No. FA9550-09-1-0283.

APPENDIX: DETERMINATION OF $\langle \nabla \Psi_i \rangle$

The average image-charge force is defined as

$$\langle \nabla \psi_i \rangle = \frac{1}{N_b} \int (\nabla \psi_i) n_b(\mathbf{r}) d\mathbf{r}. \quad (\text{A1})$$

For the sake of simplicity and without loss of generality, we choose the x -axis to be along the direction of the centroid displacement from the system symmetry axis, i.e., $\mathbf{r}_0=r_0\hat{\mathbf{x}}$. Given that, the image charge that describes the conductor effects is located along the same axis, at $\mathbf{r}_i=r_i\hat{\mathbf{x}}$, with $r_i \equiv r_w^2/r_0$. In Cartesian coordinates Eq. (A1) becomes

$$\langle \nabla \psi_i \rangle = \frac{\gamma_b^2 K}{N_b} \int \frac{(x-r_i)\hat{\mathbf{x}} + y\hat{\mathbf{y}}}{(x-r_i)^2 + y^2} n_b(x,y) dx dy, \quad (\text{A2})$$

where use has been made of Eq. (3). Since the beam distribution is assumed to be axisymmetric with respect its centroid, it is convenient to use polar coordinates (ρ, ϕ) centered at \mathbf{r}_0 , defined by

$$x = r_0 + \rho \cos \phi, \quad (\text{A3})$$

$$y = \rho \sin \phi. \quad (\text{A4})$$

It is clear that in these coordinates, the beam density is a function of ρ only, i.e., $n_b(\mathbf{r})=n_b(\rho)$, and

$$\begin{aligned} \langle \nabla \psi_i \rangle &= \frac{\gamma_b^2 K}{N_b} \int n_b(\rho) \rho d\rho \\ &\times \int_0^{2\pi} \frac{(\rho \cos \phi - a)\hat{\mathbf{x}} + \rho \sin \phi \hat{\mathbf{y}}}{a^2 + \rho^2 - 2a\rho \cos \phi} d\phi, \end{aligned} \quad (\text{A5})$$

where $a=r_i-r_0$ is the distance between the image-charge and the centroid. Performing the integration over ϕ , we readily obtain

$$\langle \nabla \psi_i \rangle = -\frac{2\pi\gamma_b^2 K}{aN_b} \int n_b(\rho) \rho d\rho \hat{\mathbf{x}} = -\frac{\gamma_b^2 K}{a} \hat{\mathbf{x}}, \quad (\text{A6})$$

where use has been made of $2\pi \int n_b(\rho) \rho d\rho = \int n_b(\mathbf{r}) d\mathbf{r} = N_b$. Equation (A6) shows that the interaction between centroid and its image is equivalent to the force of two attracting lines of charge separated by the distance a . Using $r_i=r_w^2/r_0$ and $r_0\hat{\mathbf{x}}=\mathbf{r}_0$, we can finally write

$$\langle \nabla \psi_i \rangle = -\frac{\gamma_b^2 K \mathbf{r}_0}{r_w^2 - r_0^2}. \quad (\text{A7})$$

Expanding this result to linear order in r_0 we obtain $\langle \nabla \psi_i \rangle = -\gamma_b^2 K \mathbf{r}_0 / r_w^2$, which is used to obtain Eq. (5).

- ¹Proceedings of the 11th European Particle Accelerator Conference, edited by I. Andrian, O. Brüning, Ch. Petit-Jean-Genaz, and P. Pierini (EPS-AG, Genoa, Italy, 2008).
- ²IEEE Trans. Plasma Sci. **36** (2008), the 12th special issue on high-power microwave generation, edited by J. Luginsland, J. Sirigiri, and J. Yater.
- ³M. Hess and C. Chen, *Phys. Plasmas* **7**, 5206 (2000); *Phys. Lett. A* **295**, 305 (2002); *Phys. Rev. ST Accel. Beams* **7**, 092002 (2004).
- ⁴J. S. Moraes, R. Pakter, and F. B. Rizzato, *Phys. Rev. Lett.* **93**, 244801 (2004); *Phys. Plasmas* **12**, 023104 (2005).
- ⁵M. Hess, *IEEE Trans. Plasma Sci.* **36**, 729 (2008).
- ⁶K. Fiuzza, F. B. Rizzato, and R. Pakter, *Phys. Plasmas* **13**, 023101 (2006).
- ⁷R. A. Jameson, *AIP Conf. Proc.* **279**, 969 (1992).
- ⁸F. J. Agee, *IEEE Trans. Plasma Sci.* **26**, 235 (1998).
- ⁹M. Reiser, *Theory and Design of Charged Particle Beams* (Wiley-Interscience, New York, 1994).
- ¹⁰R. C. Davidson and H. Qin, *Physics of Intense Charged Particle Beams in High Energy Accelerators* (World Scientific, Singapore, 2001).
- ¹¹R. Pakter, Y. Levin, and F. B. Rizzato, *Appl. Phys. Lett.* **91**, 251503 (2007).
- ¹²R. Pakter, G. Corso, T. S. Caetano, D. Dillenburg, and F. B. Rizzato, *Phys. Plasmas* **1**, 4099 (1994).
- ¹³R. L. Gluckstern, W.-H. Cheng, S. S. Kurennoy, and H. Ye, *Phys. Rev. E* **54**, 6788 (1996).
- ¹⁴T. P. Wangler, K. R. Crandall, R. Ryne, and T. S. Wang, *Phys. Rev. ST Accel. Beams* **1**, 084201 (1998).
- ¹⁵C. Chen and R. Pakter, *Phys. Plasmas* **7**, 2203 (2000).
- ¹⁶R. A. Kishek, P. G. O'Shea, and M. Reiser, *Phys. Rev. Lett.* **85**, 4514 (2000).
- ¹⁷S. M. Lund and B. Bukh, *Phys. Rev. ST Accel. Beams* **7**, 024801 (2004).